

# Eutectic Temperatures For Low and High Pressure Phases of Sodium Sulfate Hydrates

A. J. Dougherty<sup>1</sup>, J.A. Avidon<sup>1</sup>, D. L. Hogenboom<sup>1</sup>, and J. S. Kargel<sup>2</sup>,

<sup>1</sup>Dept. of Physics, Lafayette College, Easton, PA 18042, e-mail: doughera@lafayette.edu, avidonj@lafayette.edu, hogenbod@lafayette.edu,

<sup>2</sup>Department of Hydrology and Water Resources, The University of Arizona, Harshbarger Building, PO Box 210011, Tucson, AZ 85721-0011, e-mail: kargel@hwr.arizona.edu

## Why Study High Pressure Phases of Sodium Sulfate?

Sodium sulfate, along with other hydrated salts such as magnesium sulfate, which we studied previously [1,2], is a likely constituent of Europa's ocean and icy shell [3,4], based on chondrite-evolution models and evidence of matches to NIMS spectra of the non-ice regions of Europa's surface. These salts could depress melting points, alter buoyancy relations of key phases, form thick layers of bedded seafloor sediments, and allow explosive aqueous eruptions. The depressed melting point might also play a role in ice lens formation beneath Europa's chaos terrain [5]. It is therefore useful to know the high pressure and low temperature phase behavior of these minerals. In addition, sodium sulfate minerals are common terrestrial evaporite phases, and are probably abundant on Mars [6-8].

## Background

The three main solid phases of  $\text{Na}_2\text{SO}_4$  are the anhydrous thenardite, the heptahydrate ( $\text{Na}_2\text{SO}_4 \cdot 7\text{H}_2\text{O}$ ), and mirabilite ( $\text{Na}_2\text{SO}_4 \cdot 10\text{H}_2\text{O}$ ) [9-13]. For the concentration of 15.5 wt.% used in this experiment, mirabilite is the stable state, though long-lived metastable states of the heptahydrate have been reported [12,13].

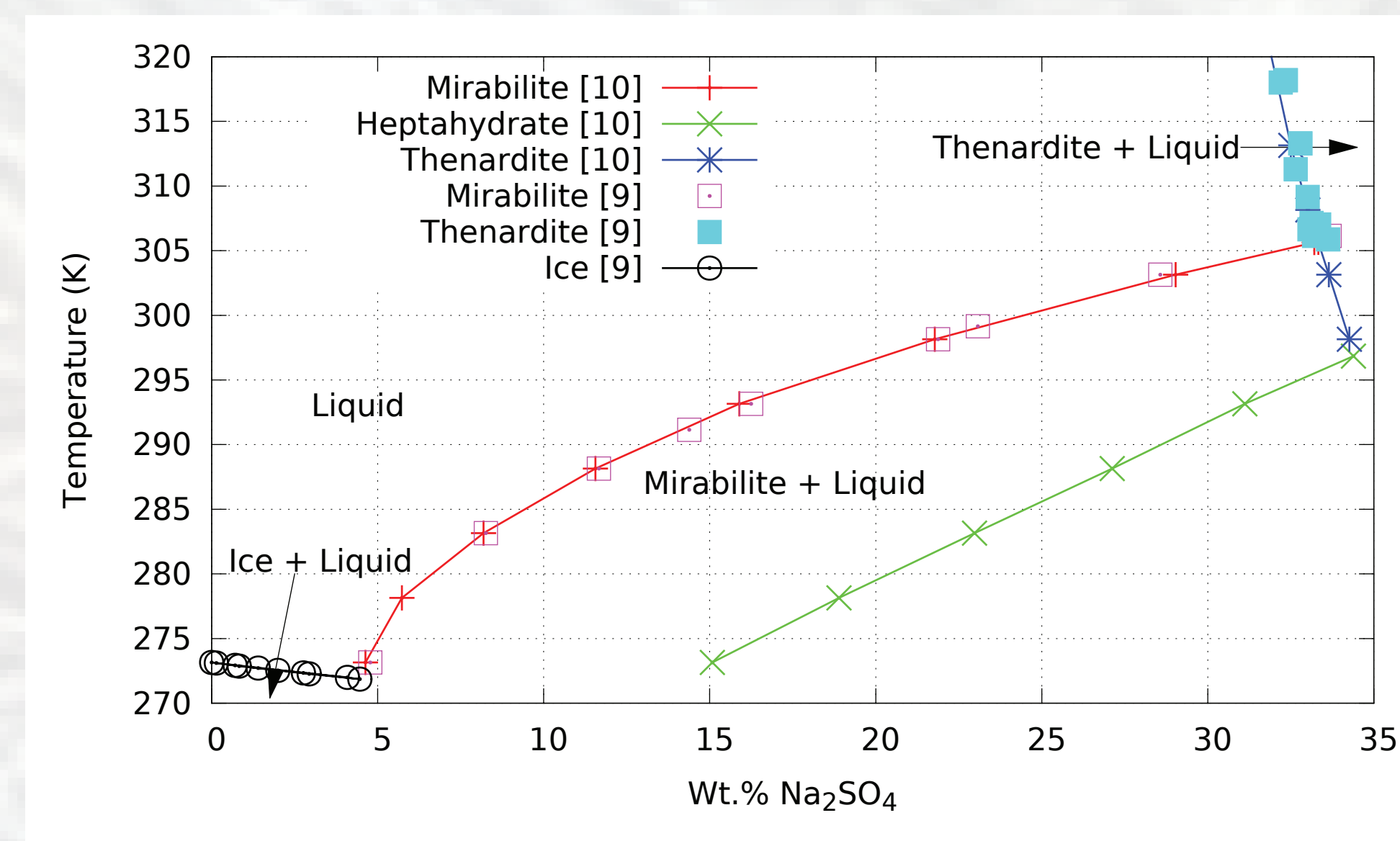


**Figure 1: Phase diagram for  $\text{Na}_2\text{SO}_4 \cdot n\text{H}_2\text{O}$  at atmospheric pressure [9-10]. For the concentration of 15.5 wt.% used in this experiment, mirabilite is the expected stable crystal form.**

## Experimental Apparatus

The apparatus consists of 3 main parts: a central high-pressure fitting containing the sample fluid, an optical system for imaging the sample, and a pressure system that includes both pressure and volume sensors. About one mL of sample is contained in the pressure cell, made from a standard high-pressure fitting called a cross. This stainless steel block has four ports. Two opposing ports contain replaceable plugs that have sapphire windows sealed with epoxy. The third port contains a plug in which a silicon diode thermometer is installed, and the fourth port connects the cell to the pressure system.

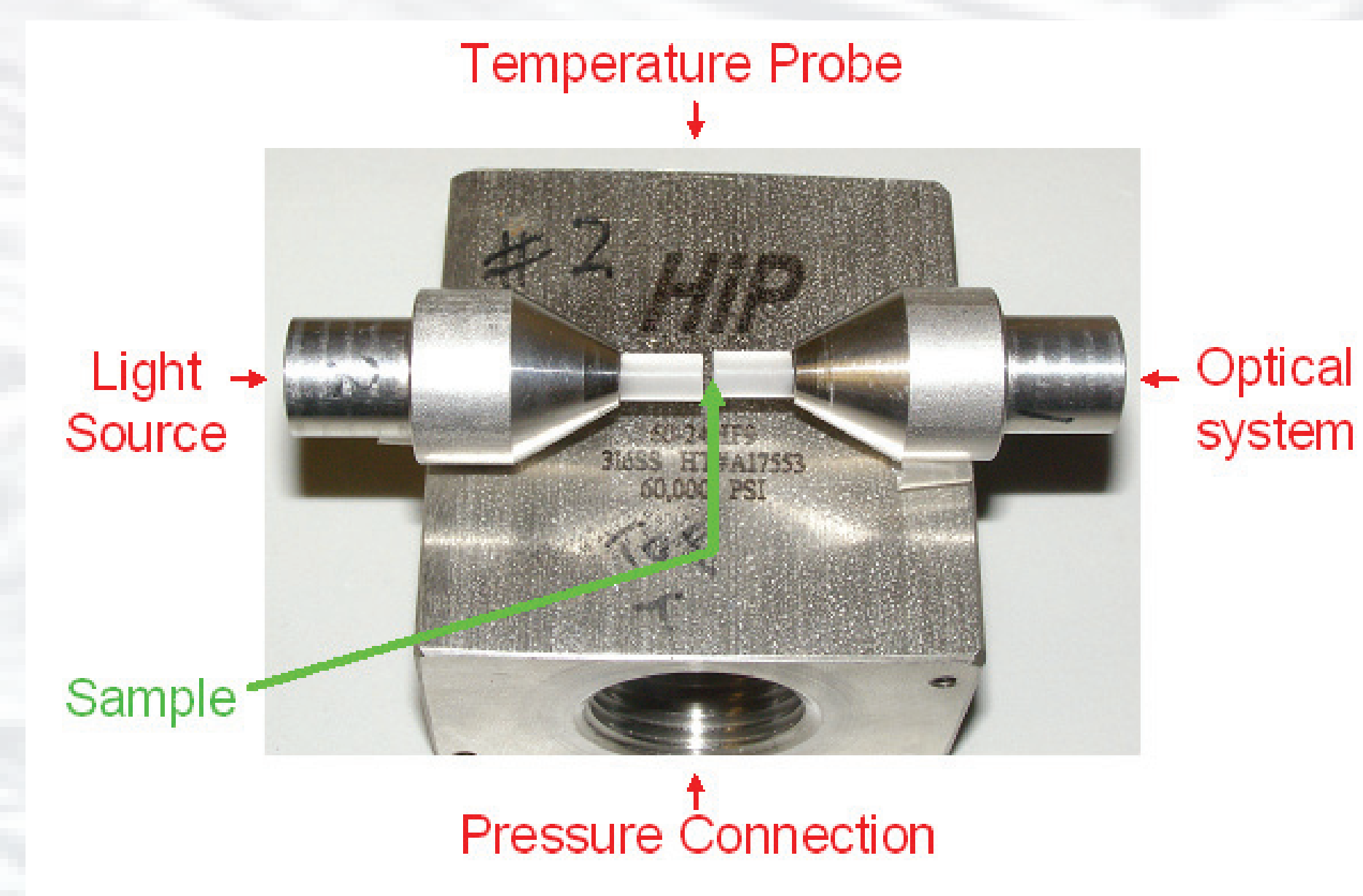


**Figure 2: Exploded view of the pressure cell. Sapphire windows in steel plugs are mounted inside a steel cross. The image shows the relative positions of the plugs with windows and the plug containing the thermometer. The window separation is approximately 1 mm.**

Collimated light enters the pressure cell through an optical fiber on the left. The image is then relayed through a microscope objective into a CCD camera. The bottom port of the cross is connected to a pipe filled with mercury that connects to the pressure system. As the sample expands or contracts, the vertical height of a magnet floating on top of the mercury is monitored with a transducer. Changes in transducer voltage are approximately proportional to changes in sample volume.

## Determining the Eutectic Temperature

The results for a run at 250 MPa are shown in Fig. 4. The system was initially pressurized to 250 MPa and warmed to point (a) so that the system was a homogeneous liquid. We then supercooled the sample to 271 K (b). The volume decreased due to thermal contraction.

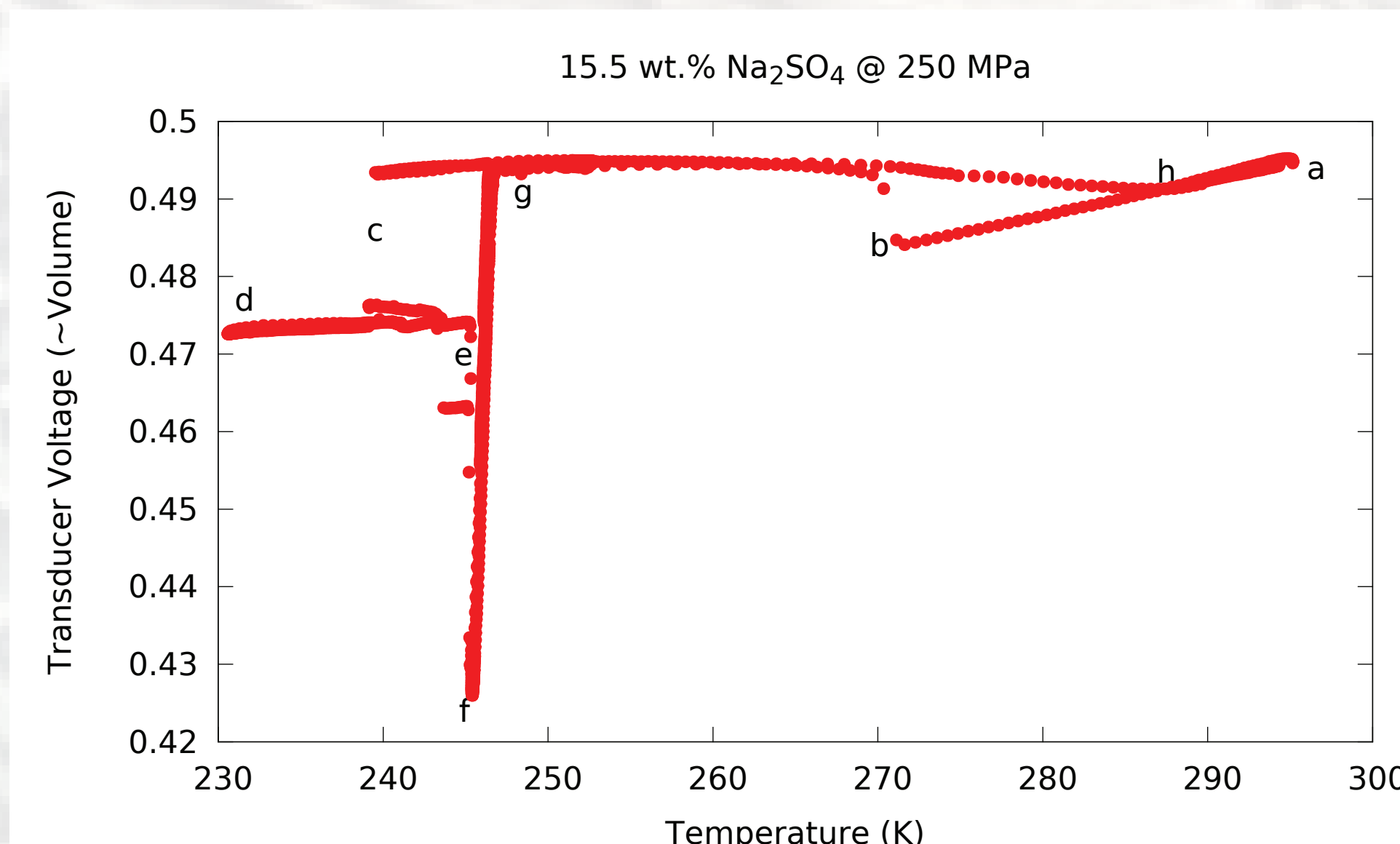


**Figure 3: Results for 250 MPa. The eutectic temperature is 246 K.**

Rapid crystallization at (b) led to a sharp increase in volume and a small increase in temperature due to the exothermic release of heat of crystallization. Although the crystals are denser than the original solution, the remaining water-rich solution is less dense, leading to a slight overall increase in volume.

The crystals continued to grow as we cooled to 239.5 K. At point (c), the remaining sample solidified rapidly. Further cooling to (d) produced no significant changes. Upon warming to (e), incipient melting or softening of the sample allowed pressure equilibrium to be re-established, thus causing a reduction in volume from (e) to (f). Reversible eutectic melting occurred from (f) to (g) near 246 K; the volume increased rapidly, and crystals were seen melting in the window.

Finally, the sample was gradually warmed to point (h), at which point the last crystals dissolved.

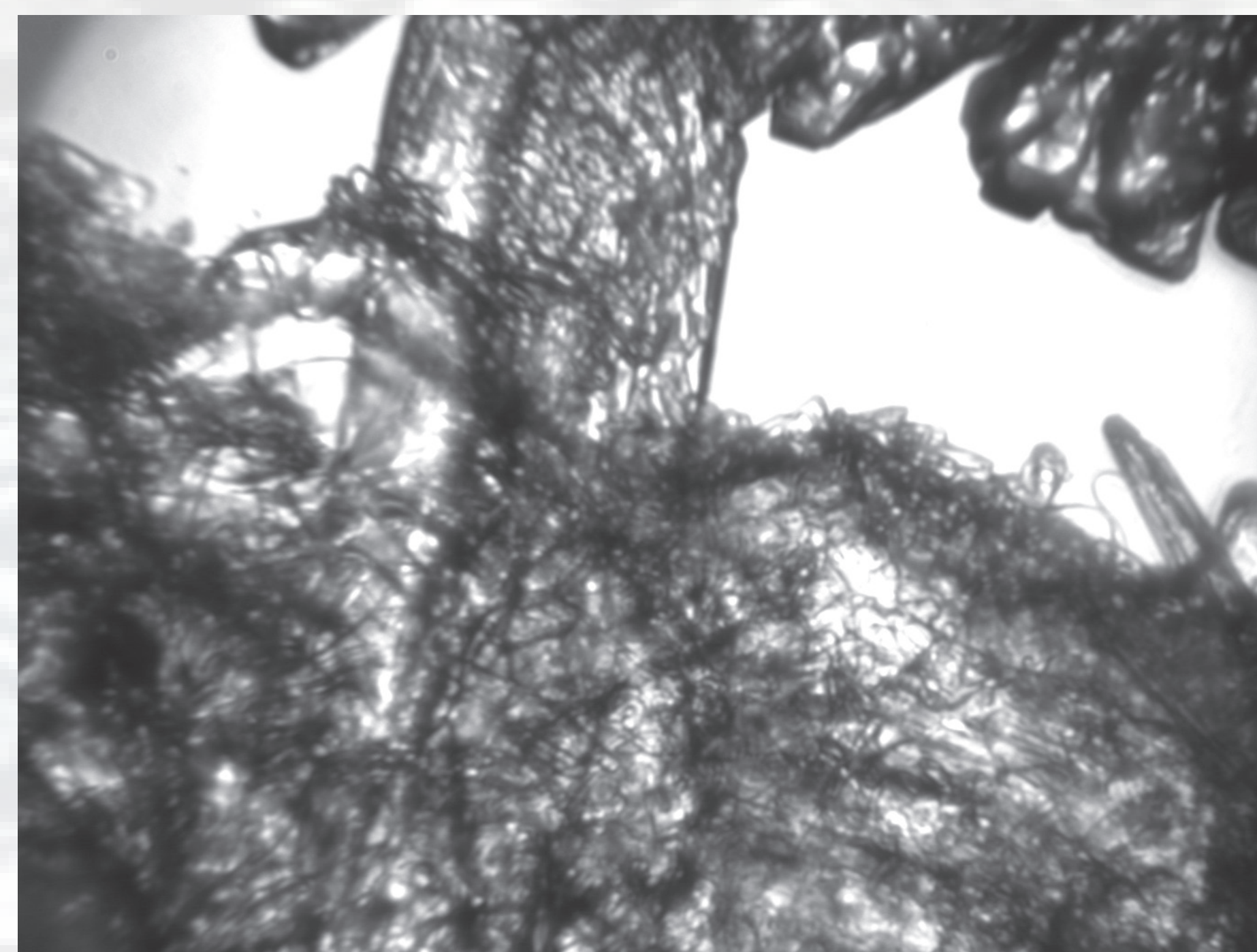


**Figure 4: Coexistence of liquid and solid during eutectic melting at  $T = 249.53 \text{ K}$ ,  $p = 295 \text{ MPa}$  (on curve Eutectic-IIIb) in Fig. 5. The image is approximately 1 mm across.**

## Methanol-Water Solutions

We have begun investigating the properties of methanol/water mixtures at low temperature and high pressure. These studies are intended to complement rheological studies of this same system [15], as a preliminary step towards studying mixtures potentially involved in cryovolcanic processes. For our initial trials, we are studying how the solubility of methanol varies as a function of pressure. Specifically, for a 40% methanol solution, we are looking at the variation of the liquidus temperature (similar to point (h) in Fig. 3 above) as a function of pressure.



The preliminary results for pressures up to 150 MPa are shown in Fig. 7. The liquidus temperature gradually decreases with increasing pressure.

**Figure 6: Ice dendrites growing at  $T = 225.77$ ,  $p = 49 \text{ MPa}$ , in a methanol-water solution.**

## Results

The eutectic temperature as a function of pressure is shown in Fig. 5. Below 209 MPa, the addition of the salt results in a small depression of the freezing point that ranges from  $\sim 0.85 \text{ K}$  at low pressure to  $\sim 1.5 \text{ K}$  near 200 MPa.

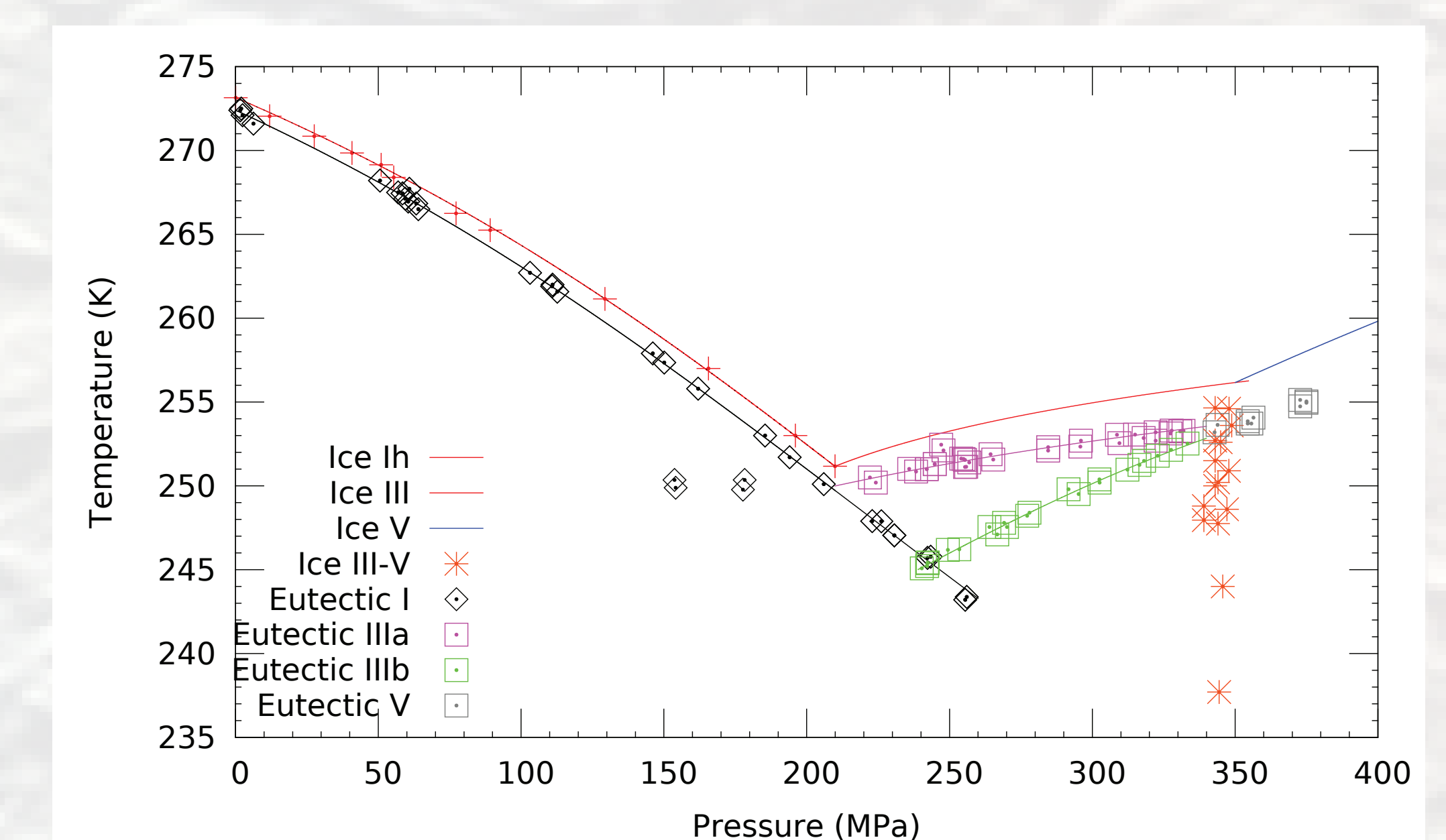


**Figure 5: Eutectic temperature as a function of pressure. The transition temperatures for various phases of ice from Ref. [14] are included for comparison.**

Above 209 MPa, the results are more complex. In most trials (purple, indicated by 'Eutectic IIIa') the freezing point depression was relatively small, but increased gradually with pressure. The density of the sample increased upon freezing, consistent with an Ice-III eutectic with mirabilite.

In some cases (green, labeled as 'Eutectic IIIb') the eutectic temperature was considerably lower (but still well above the Ice II transition). This state was also denser than the IIIa phase. We speculate that it is a eutectic mixture of Ice-III and the heptahydrate.

The IIIa and IIIb lines converge near the Ice III-V boundary. Above 350 MPa, we only observed one phase. Finally, if we started below 209 MPa with existing Ice Ih crystals and gradually increased the pressure while decreasing the temperature, we obtained the additional points labeled 'Eutectic I' in Fig. 7. The volume expanded upon freezing, and the eutectic temperatures followed the extrapolation of the low-pressure eutectic line.

Above 209 MPa, both the Eutectic-I and Eutectic-IIIb phases are metastable. By varying the temperature and pressure, the system eventually solidifies as the Eutectic-IIIa phase, presumably mirabilite.

In all cases, the phase changes are accompanied by significant volume changes, and characterizing such changes may help in the development of models of Europa's ocean and icy shell.

## References

- [1] Dougherty, A.J., Hogenboom, D.L., and Kargel, J.S. (2007) LPS XXXVIII, Abstract #2275.
- [2] Hogenboom, D.L. et al. (1995) Icarus 115:258-277.
- [3] McCord, T.B. et al. (1998) Science, 280, 1242.
- [4] Kargel, J.S. et al. (2000) Icarus 148, 226-265.
- [5] Schmidt, B.E., Blandish, D.D., Patterson, G.W., and Schenk, P.M. (2011) Nature, 479, 502.
- [6] Squyres, S.W. et al. (2004) Science, 306.
- [7] Mangold N, Gendrin A, Gondet B, et al. (2008) Icarus 194, 519-543.
- [8] Kargel, J.S., Furfaro, R., Prieto-Ballesteros, O., Rodriguez, J.A.P., Montgomery, D.R., Gillespie, A.R., Marion, G.M., Wood, S.E. (2007) Geology, 35, 975-978.
- [9] Wuite, J.P. (1913) Z. Physik. Chem. 86, 349-382.
- [10] Eddy R.D. and Menzies A.W. (1940) J. Phys. Chem, 44, 207-235.
- [11] Hartley et al. (1908) J. Chem. Soc. Trans. 93:825-833.
- [12] Hall, C. and Hamilton, A. (2008) Icarus, 198 (1): 277-279.
- [13] Hamilton, A. (2008) Journal of Physics D-Applied Physics, 41, 212002.
- [14] Bridgman, P.W. (1911) Proc. Amer. Acad. Arts Sci. 47, 441.
- [15] Zhong, F., Mitchell, K.L., Hays, C.C., Choukroun, M., Barmatz, M., and Kargel, J.S. Icarus, 202 (2009) 607-619.

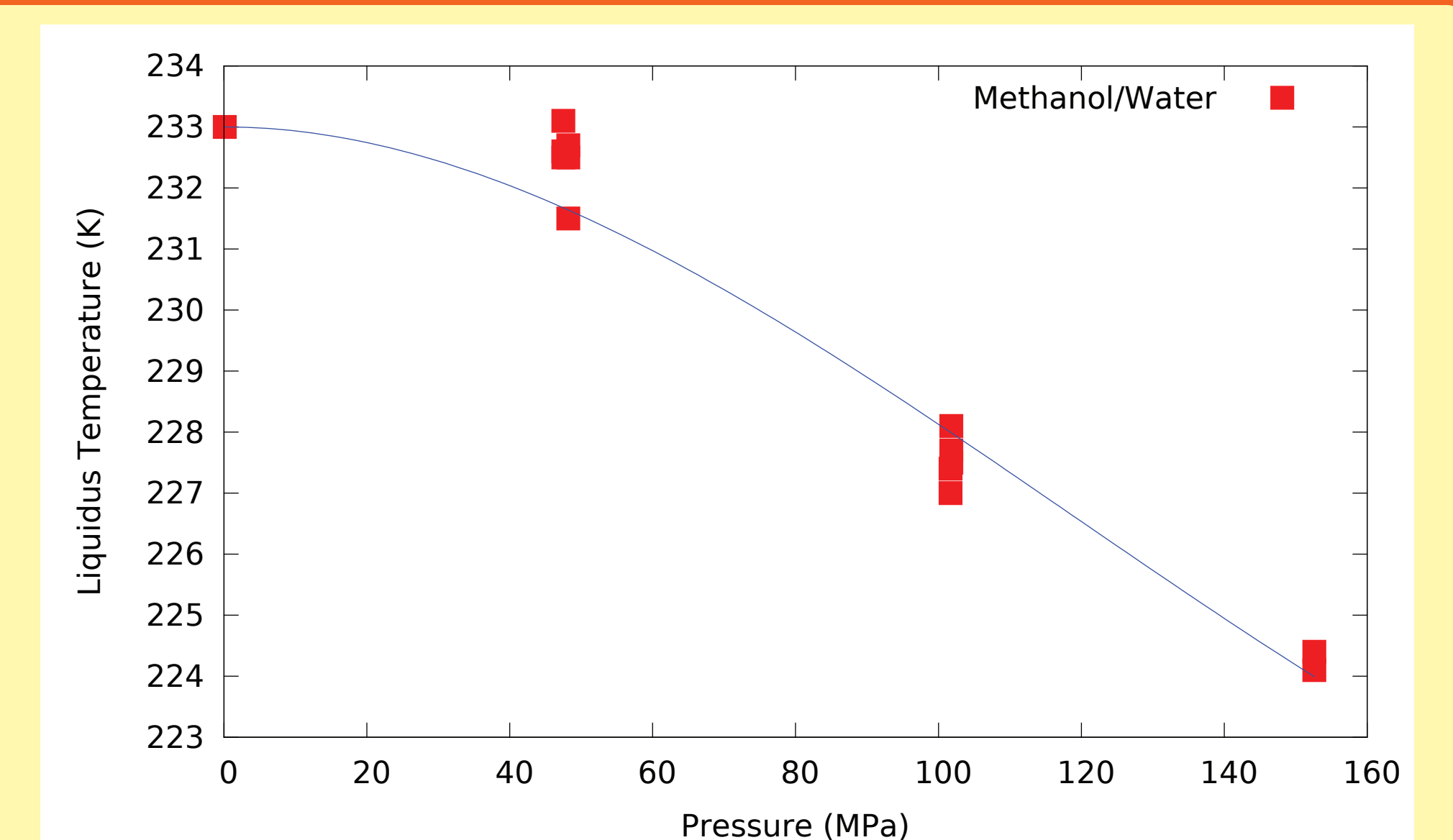


**Figure 7: Liquidus temperature as a function of pressure for a 40% methanol/water solution.**

In future work, we plan to refine these measurements and extend them to higher pressures in the Ice-III regime. We then will consider other solutions, such as ammonia-water, that are likely to be important for the icy bodies of the outer solar system.